Available online at www.sciencedirect.com
ScienceDirect
Journal of Organometallic Chemistry 693 (2008) 1186–1194
Journal of Organometallic Chemistry
www.elsevier.com/locate/jorganchem

Diaza-18-crown-6 based chromophores for modulation of two-photon absorption cross-section by metal ions

Atanu Jana, Arijit Kumar De, Amit Nag, Debabrata Goswami, Parimal K. Bharadwaj *

Department of Chemistry, Indian Institute of Technology, Kanpur 208016, India

Received 10 October 2007; received in revised form 28 December 2007; accepted 8 January 2008
Available online 17 January 2008

Abstract

Two chromophores with diaza-18-crown-6 as receptor have been synthesized in high yields. The electronic structure, one-photon absorption (OPA) spectra, and two-photon absorption (TPA) properties have been studied in detail. When no metal ion is added as input, both show negligible TPA cross-section (σ_2). However, in the presence of Zn(II)/Cd(II)/Mg(II)/Ca(II) ion, each exhibits large TPA cross-section value. Binding of metal ion in the receptor increases the symmetric charge transfer leading to large σ_2 values. Theoretical calculations at the B3LYP functional with 6-31G* and LanL2DZ mixed basis set under DFT formalism support experimental results.

Keywords: Aza-crown ether receptor; Charge transfer; DFT; OPA; TPA

1. Introduction

Molecules that exhibit optical nonlinearity are presently in demand as they are potentially useful in opto-electronics as well as all-optical data processing technologies. Third-order optical nonlinearity of molecules measured in terms of two-photon absorption cross-section (σ_2) is particularly important in bio-photonics and materials science such as photodynamic therapy [1], optical power limiting [2], three-dimensional optical data storage [3], two-photon up-conversion lasing [4], and so on. Besides, modulation of TPA activity of molecules in the presence of certain ions are important from the perspectives of detection and determination of static concentration of these ions in bio-systems which is important in understanding of biological processes. An important class of compounds capable of exhibiting large TPA cross-section are organic molecules with symmetrical charge transfer possibilities. When a metal ion influences this charge transfer, modulation of the TPA activity can be achieved. It should be noted, however, that TPA enhancement rather than its lowering in the presence of a metal ion will be better understood. With this design principle in mind, we have attached 4-(dimethylamino)benzene or ferrocene group to diaza-18-crown-6 to have two D–π–D′ moieties symmetrically disposed (Scheme 1).

Crown ethers can bind biologically relevant alkali and alkaline earth metal ions while mixed aza-oxa crown ethers can complex other types of metal ions as well. Diaza-18-crown-6 is a good receptor for Zn(II), Cd(II) and Mg(II) ions in addition to alkali metal ions such as Na(I) and K(I). Zinc is an essential nutrient required in normal growth and development [5] and for cellular processes such as DNA repair [6] and apoptosis [7]. This metal plays a key role in the synthesis of insulin and the pathological state of diabetes [8]. On the other hand, many enzymatic reactions are mediated by Mg(II) while Ca(II) acts as a universal second messenger in cells [9].

Metal ions are excellent 3D templates and can assemble simple organic NLO-phores around with concomitant tuning of the molecular nonlinear optical properties by virtue of inducing a strong intra-ligand charge transfer (ILCT) transition. There are very few examples on the metal ion

* Corresponding author.
E-mail address: pkb@iitk.ac.in (P.K. Bharadwaj).

0022-328X/$ - see front matter © 2008 Elsevier B.V. All rights reserved.
doi:10.1016/j.jorganchem.2008.01.019

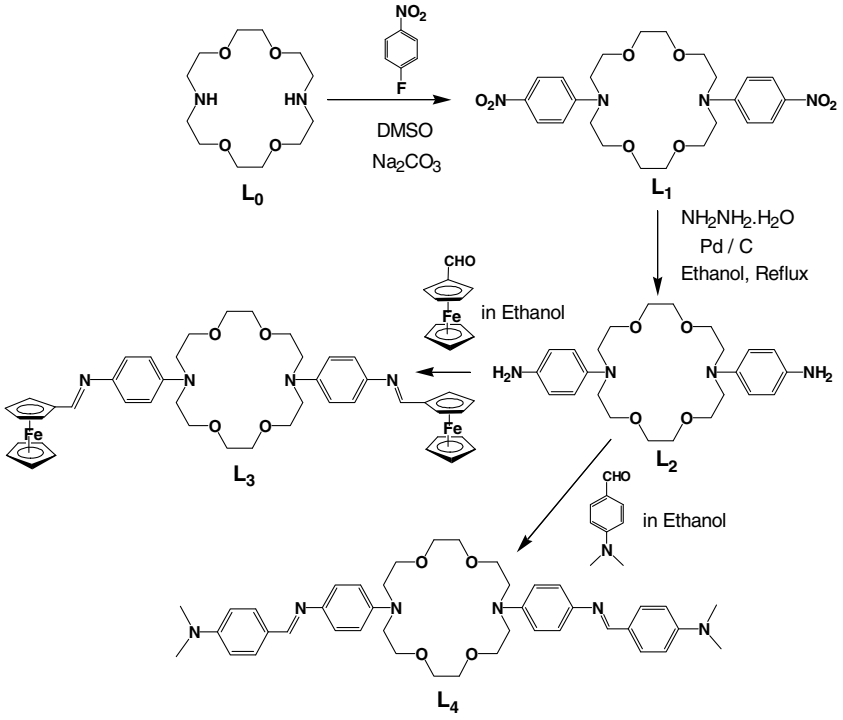

Scheme 1. Synthetic scheme for the chromophores $\mathbf{L}_3$ and $\mathbf{L}_4$ studied in this work.

induced TPA cross-section reported earlier in the literature [10]. Herein, the NLO-phores $\mathbf{L}_3$ and $\mathbf{L}_4$ are designed such that in absence of a metal ion, the two D–π–D′ units present in each compound, are electronically independent. When a metal ion occupies the cavity, it can electronically connect the two D–π–D′ moieties into D–π–A–π–D leading to increased symmetry of charge transfer and hence larger TPA cross-section. Theoretical calculations were carried out to support the experimental findings.

2. Experimental

2.1. Materials

Reagent grade 1,4,10,13-tetraoxa-7,16-diazacyclooctadecane, 1-fluoro-4-nitrobenzene, 4-(dimethylamino)benzaldehyde, ferrocene carboxaldehyde, 10% Pd in activated charcoal, Rhodamine-6G and all the metal perchlorate salts were acquired from Aldrich (USA) and used as received. Reagent grade hydrazine hydrate, Na_2CO_3 and the solvents were purchased from SD Fine Chemicals (India). The solvents were purified before use following established methods. All the reactions were carried out under dinitrogen atmosphere unless otherwise mentioned. Chromatographic separations were achieved by column chromatography using neutral alumina from Acme Chemicals (India).

2.2. Synthesis of ligands

The synthesis of the compounds was achieved in several stages as illustrated in Scheme 1. One or two *p*-nitrobenzene groups can be grafted by simple aromatic nucleophilic substitution (ArSN) reaction that on reduction affords the corresponding amines that can readily undergo Schiff base condensation with aldehydes leading to the target compounds.

2.2.1. Synthesis of N,N′-bis(4-nitrophenyl)-4,13 diaza-18-crown-6 derivative ($\mathbf{L}_1$)

To a solution of 1,4,10,13-tetraoxa-7,16-diaza cyclooctadecane, $\mathbf{L}_0$ (1 g; 3.8 mmol) in dry DMSO (15 mL) was added anhydrous Na_2CO_3 (1.0 g; 9.5 mmol). Subsequently, 1-fluoro-4-nitrobenzene (0.9 mL; 8.7 mmol) in dry DMSO (15 mL) was added drop wise in 30 min and the reaction mixture was allowed to stirred at 80 °C for 72 h. It was then poured into ice water (250 mL). The separated yellow solid was collected by filtration and washed thoroughly with water (5 × 100 mL). This yellow solid contains a mixture of mono- as well as bis-derivative with some excess of 1-fluoro-4-nitrobenzene and was separated by column chromatography (neutral alumina). After removing the impurities, the bis-derivative ($\mathbf{L}_1$) was eluted first using hexane: EtOAc (55:45 v/v) as the eluent. After evaporating the solvent, the yellow solid was recrystallized from MeCN to obtain a bright yellow crystalline solid. Yield: ~60%; m.p. 205 °C. ^{1}H NMR spectra (400 MHz, $CDCl_3$, TMS, 25 °C) δ: 3.41–3.94 (m, 24H), 6.02 (d, $J = 9.5$ Hz 6H), 8.08 (d, $J = 9.4$ Hz, 4H); ^{13}C NMR spectra (100 MHz, $CDCl_3$) δ: 51.7, 68.7, 71.1, 110.3, 126.2, 137.6, 152.7; ESI-MS (*m*/*z*): 527 (100%) $[M+Na]^+$. Anal. Calc. for $C_{24}H_{32}N_4O_8$: C, 57.13; H, 6.39; N, 11.10. Found: C, 56.98; H, 6.31; N, 11.19%.

2.2.2. Synthesis of N,N′-bis(4-aminophenyl)-4,13 diaza-18-crown-6 derivative (L_2)

The nitro-compound obtained above was reduced to the corresponding amine by hydrazine hydrate in the presence of Pd–C catalyst in refluxing ethanol [11]. Typically, the bis-nitro derivative (L_1) (0.8 g; 1.6 mmol) was taken in a two necked round bottom flask with 50 mL absolute ethanol, added 0.015 g of 10% Pd in activated charcoal followed by hydrazine hydrate (2.6 mL) over a period of 30 min and the mixture was refluxed for 3 h. It was filtered hot and then evaporated almost to dryness. The mixture was shaken with 100 mL water to remove excess hydrazine hydrate and the desired amine extracted with chloroform, dried over anhydrous Na_2SO_4 and finally evaporated to obtain the product as a colorless semi-solid. Yield: ~65%; ^{1}H NMR spectra (400 MHz, $CDCl_3$, TMS, 25 °C) δ: 3.4–3.67 (m, 24H), 3.89 (b, 4H), 6.55–6.71 (m, 8H); ^{13}C NMR spectra (100 MHz, $CDCl_3$) δ: 52.8, 69.1, 70.7, 116.2, 117.2, 137.4, 141.3; ESI-MS (m/z): 445 (40%) $[MH]^+$. Anal. Calc. for $C_{24}H_{36}N_4O_4$: C, 64.84; H, 8.16; N, 12.60. Found: C, 64.73; H, 7.91; N, 12.48%.

2.2.3. Synthesis of the chromophores (L_3 and L_4)

The NLO-phores were synthesized by Schiff base condensation of the amine with an equivalent amount of either 4-(dimethylamino)benzaldehyde or ferrocene carboxaldehyde in dry ethanol. The desired product precipitated out on stirring at RT for 24 h. This was collected by filtration, washed twice with dry ethanol followed by diethyl ether and finally dried in vacuo. These compounds were directly used for analysis and further studies. All attempts to make single crystals of any of these compounds remained unsuccessful.

L_3: Yield ~85%; m.p. 165 °C; ^{1}H NMR spectra (400 MHz, $CDCl_3$, TMS, 25 °C) δ: 3.58–3.71(m, 24H), 4.17(s, 10H), 4.4(d, $J = 10.6$ Hz, 4H), 4.71(d, $J = 9.0$ Hz, 4H), 6.63(d, $J = 9.0$ Hz, 2H), 7.02–7.09 (m, 6H), 8.26 (d, $J = 5.9$ Hz, 2H); ^{13}C NMR spectra (100 MHz, $CDCl_3$) δ: 48.8, 51.4, 68.6, 69.0, 69.1, 69.2, 69.6, 70.1, 70.2, 70.8, 71.3, 112.0, 121.3, 121.9, 122.2, 141.6, 161.4; ESI-MS (m/z): 837(30%) $[M]^+$, 878 (100%) $[M+MeCN]^+$. Anal. Calc. for $C_{46}H_{52}N_4O_4Fe_2$: C, 66.04; H, 6.26; N, 6.69. Found: C, 65.93; H, 6.48; N, 6.43%.

L_4: Yield ~65%; m.p. 150 °C; ^{1}H NMR spectra (400 MHz, $CDCl_3$, TMS, 25 °C) δ: 3.01 (s, 6H), 3.03 (s, 6H), 3.64–3.76 (m, 24H), 6.66–6.72 (m, 6H), 7.06–7.18 (m, 6H), 7.71–7.74 (m, 4H), 8.27 (d, $J = 4.6$ Hz, 2H); ^{13}C NMR spectra (100 MHz, $CDCl_3$) δ: 40.2, 51.5, 69.0, 70.7, 70.9, 111.6, 112.1, 121.6, 122.2, 129.9, 130.4, 146.0, 151.9, 160.3; ESI-MS (m/z): 707 (25%) $[M]^+$, 748 (100%) $[M+MeCN]^+$. Anal. Calc. for $C_{42}H_{54}N_6O_4$: C, 71.36; H, 7.69; N, 11.89. Found: C, 71.23; H, 7.39; N, 11.99%.

2.3. Methods

All the compounds were characterized by elemental analysis, NMR, and ESI-MS spectra. Both ^{1}H NMR (400 MHz) and ^{13}C NMR spectra (100 MHz) of the compounds were recorded on a JEOL JNM-LA400 FT spectrometer in $CDCl_3$ with tetramethylsilane as internal standard. Melting points were measured with an electrical melting point apparatus by PERFIT, India and were uncorrected. Elemental analyses were recorded in an Elementar Vario EL III Carlo Erba 1108 Elemental Analyser. The ESI-MS data were obtained from a MICROMASS QUATRO Quadruple Mass Spectrometer. Each sample dissolved in acetonitrile and introduced into the ESI source through a syringe pump at the rate of 5 μl/min. The ESI capillary was set at 3.5 kV and the cone voltage was 40 V. The spectra were collected in 6 s scans and the printouts were averaged of 6–8 scans. Microanalyses for the compounds were obtained from CDRI, Lucknow, India. UV–vis spectra were recorded on a JASCO V570 UV–vis–NIR spectrophotometer in dry acetonitrile at 298 K.

2.3.1. Measurement of two-photon absorption cross-section (σ_2)

Two-photon absorption cross-section measurements were carried out by open-aperture Z-scan technique [12] in the wavelength range of 750–850 nm in 10^{-4} M dry acetonitrile solution of the chromophores and their metal complexes.

The femtosecond experimental scheme involves modelocked Coherent Mira titanium: sapphire laser (Model 900) which is pumped by Coherent Verdi frequency doubled Nd: vanadate laser. The model 900 Mira is tunable from 740 to 900 nm and its repetition rate is 76 MHz. The duration of the pulse was 150 fs as measured by autocorrelation technique. Using a 20 cm focal length lens, the beam was focused into a 1 mm long cell filled with sample, where it easily produces GW-level intensity at the focal point of the lens. The sample was scanned through the focal point using a motorized translation stage (model ESP 300), which can step with a minimum resolution of 0.1 μm. This allows a smooth intensity scan for the samples in this wavelength. The transmitted beam, after passing through the sample was focused into the aperture of a UV-enhanced amplified silicon photo detector (Thorlabs DET 210) by using a 7.5 cm focal length lens. We measured the signal in an oscilloscope (Tektronix TDS 224), which was triggered by the chopper frequency. The signal was measured in an oscilloscope (Tektronix TDS 224), which is finally interfaced with the computer using GPIB card (National Instruments). The data was acquired using LabVIEW programming. The nonlinear absorption coefficient β was obtained [13], by fitting our measured transmittance values to the following formula:

$$T(z) = 1 - \beta I_0 L/(2(1 + z^2/z_0^2))$$

where β = nonlinear absorption coefficient, I_0 = on-axis electric field intensity at the focal point in absence of the sample, L = sample thickness, z_0 = Rayleigh range = $\pi w_0^2/\lambda$, w_0 is the minimum spot size at the focal point. The β values are obtained by curve fitting the measured

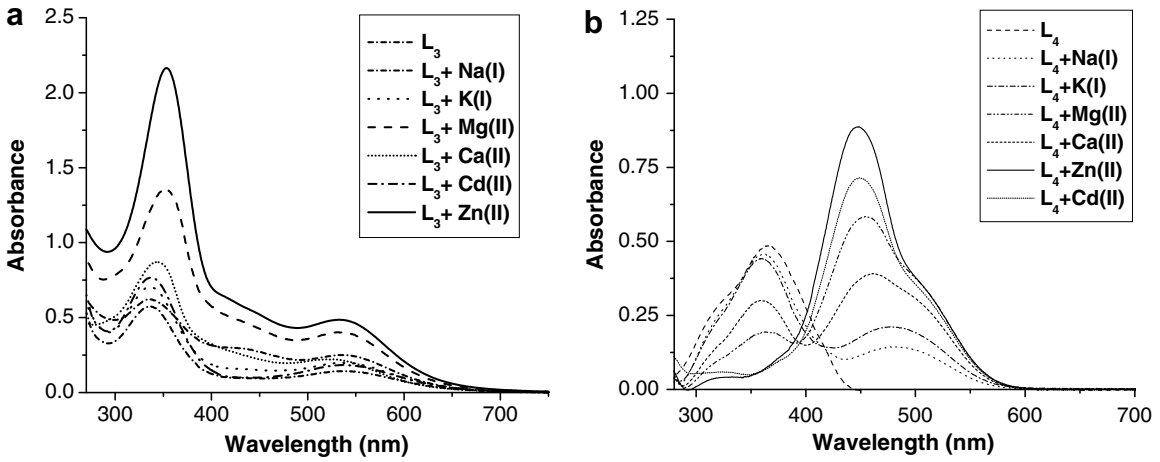

Fig. 1. (a) Single photon absorption spectra of chromophore $\mathbf{L}_3$ and their corresponding metal complexes in 10^{-5} M CH_3CN solution. (b) Single photon absorption spectra of $\mathbf{L}_4$ and their corresponding metal complexes in 10^{-5} M CH_3CN solution.

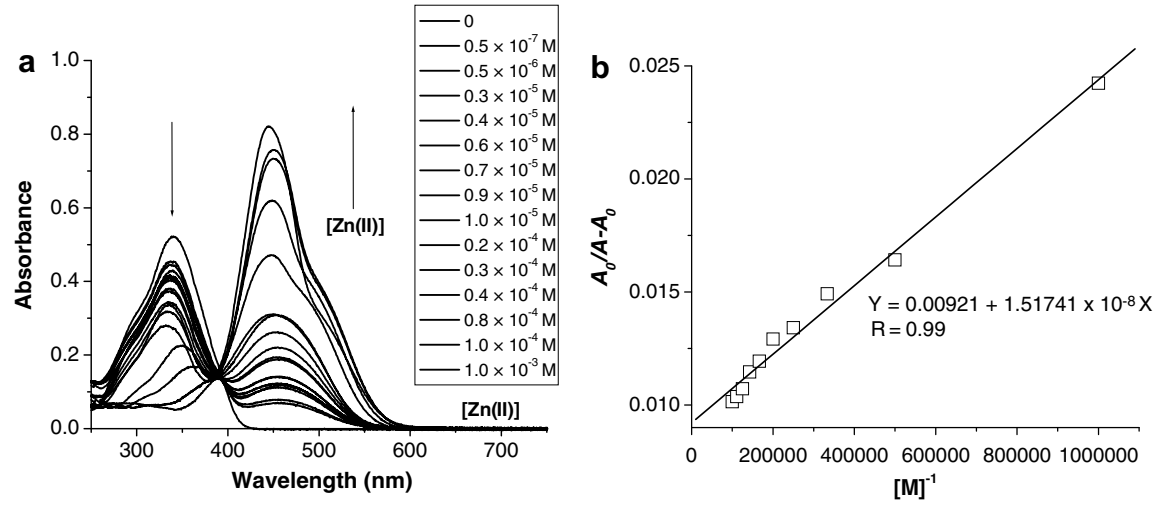

Fig. 2. (a) Absorption spectra of the chromophore $\mathbf{L}_4$ as a function of [Zn(II)]. The arrows indicate the trend for increasing [Zn(II)]. The [$\mathbf{L}_4$] is 1×10^{-5} M. (b) Plot of $A_0/A - A_0$ against $[\mathrm{Zn(II)}]^{-1}$ for binding constant determination. The absorption data yield $\log K_s = 5.783$.

open-aperture traces with the above equation. After getting the value of β, the TPA cross-section σ_2 in GM unit of one solute molecule is given by the following expression:

$$\sigma_2 = \beta h v / N \cdot c \cdot 10^{-3}$$

where v is the frequency of the incident laser beam, N is Avogadro constant, c is the concentration of the compound in CH_3CN solvent. Rhodamine 6G was taken as the reference to calibrate the measurement technique for which the σ_2 value is known in the literature [14].

2.3.2. Binding constant determination

The binding constants (K_s) for the complexes between the chromophores and metal salts were determined by UV–vis spectroscopic titration method. The concentration of the ligands was 1×10^{-5} M and that of metal ions was in the range of 1×10^{-3} M to 1×10^{-7} M. The linear fit of the absorption spectral data at a particular wavelength

Table 1
Photophysical data for the chromophores $\mathbf{L}_3$ and $\mathbf{L}_4$ and their corresponding metal complexes

Compounds	λ_{max} (nm)	$\varepsilon \times 10^4$ (mol L^{-1} cm^{-1})	Max σ_2 (GM) in the range of 750–850 nm
$\mathbf{L}_3$	334, 546	5.736, 1.426	21
$\mathbf{L}_3 + Na(ClO_4) \cdot xH_2O$	336, 539	6.251, 2.545	1399
$\mathbf{L}_3 + K(ClO_4) \cdot xH_2O$	336, 540	7.091, 2.098	1120
$\mathbf{L}_3 + Mg(ClO_4)_2 \cdot xH_2O$	352, 536	13.601, 4.101	2567
$\mathbf{L}_3 + Ca(ClO_4)_2 \cdot xH_2O$	344, 527	8.782, 2.210	2852
$\mathbf{L}_3 + Zn(ClO_4)_2 \cdot xH_2O$	354, 537	21.745, 4.989	3223
$\mathbf{L}_3 + Cd(ClO_4)_2 \cdot xH_2O$	337, 538	7.707, 1.874	2651
$\mathbf{L}_4$	365	4.899	10
$\mathbf{L}_4 + Na(ClO_4) \cdot xH_2O$	362, 482	4.562, 1.460	13
$\mathbf{L}_4 + K(ClO_4) \cdot xH_2O$	361, 481	4.469, 2.174	16
$\mathbf{L}_4 + Mg(ClO_4)_2 \cdot xH_2O$	363, 455	1.997, 5.827	62
$\mathbf{L}_4 + Ca(ClO_4)_2 \cdot xH_2O$	359, 462	3.009, 3.905	52
$\mathbf{L}_4 + Zn(ClO_4)_2 \cdot xH_2O$	446	8.854	67
$\mathbf{L}_4 + Cd(ClO_4)_2 \cdot xH_2O$	449	7.124	54

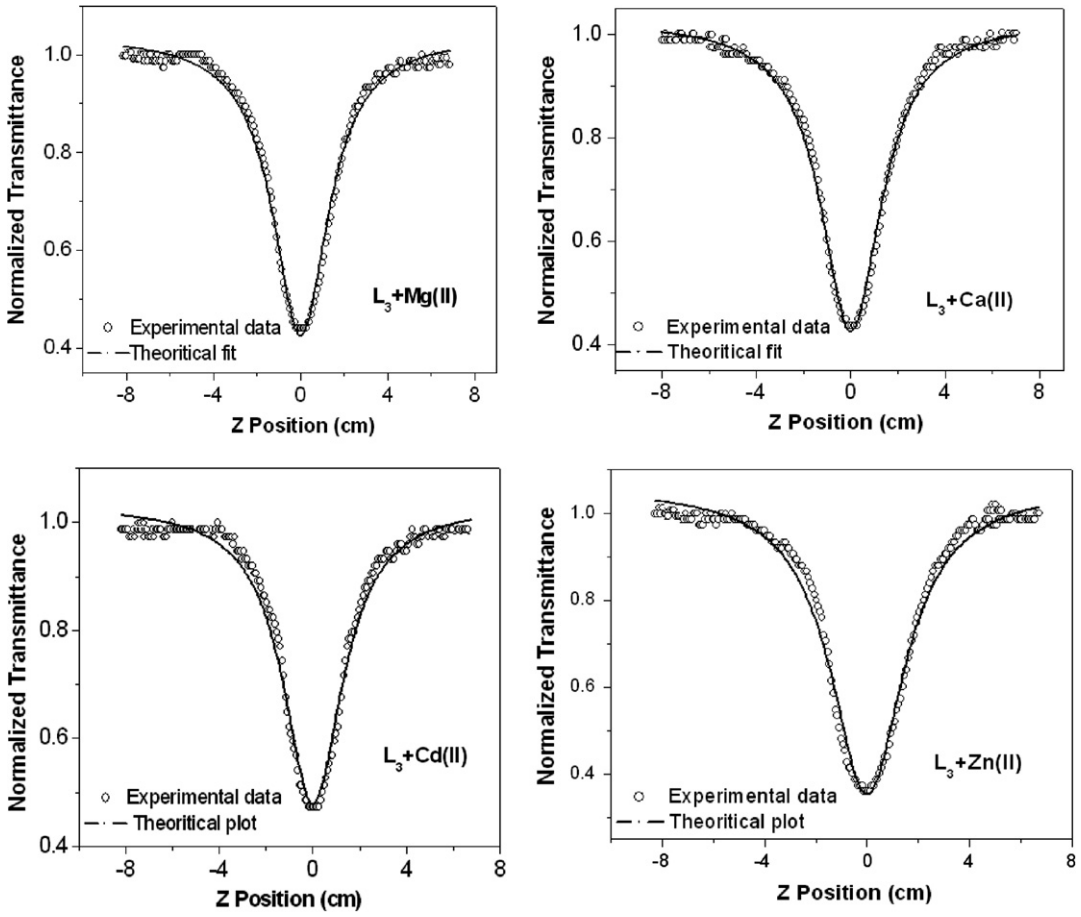

Fig. 3. Open-aperture Z-scan traces for some metal complexes of the chromophore $\mathbf{L}_3$ in 10^{-4} M CH_3CN solution. Solid lines are the best fits to the experimental data.

for 1:1 complexation was obtained by applying the following equation [15].

$$A_0/(A - A_0) = [a/(b - a)][(1/K_s[M]) + 1],$$

where A_0 and A are the absorbance of the metal-free ligand and the metal complex respectively. $[M]$ is the concentration of various metal ions added. When $A_0/(A - A_0)$ was plotted against the metal ion concentration $[M]^{-1}$, K_s was directly obtained from the intercept/slop ratio. The details of the theoretical analysis of the stoichiometries and corresponding binding constant determination are available in the literature [16]. Here the calculated values are in consistence with good correlation coefficients ($\geqslant 0.99$).

3. Results and discussion

3.1. One-photon absorption spectra of the chromophores and their corresponding metal complexes

One-photon absorption spectra for $\mathbf{L}_3$, $\mathbf{L}_4$ and their different metal complexes, taken in acetonitrile (10^{-5} M) are collected in Fig. 1. The ligand $\mathbf{L}_3$ exhibits two charge transfer bands, one at 334 nm and the other at 546 nm consistent with other ferrocenyl chromophores [17]. The 334 nm band is due to ligand-centered π–π^* electronic transition. This band makes a slight red-shift (2–15 nm) and becomes more intense in the presence of a metal ion. The lower energy band at 546 nm does not shift to any significant extent although increases in intensity along with the appearance of another weak and broad band around

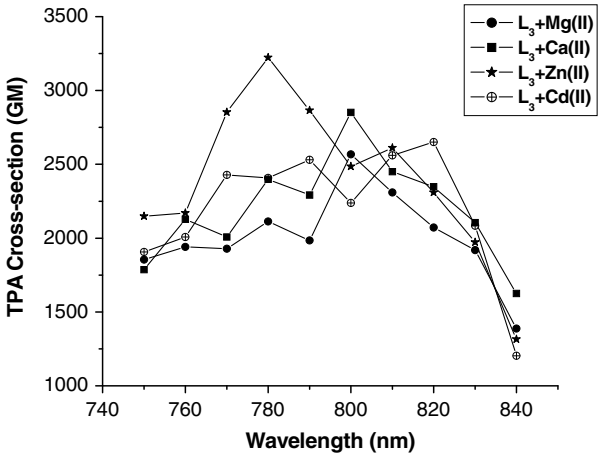

Fig. 4. Experimentally determined TPA cross-section of few metal complexes of chromophore $\mathbf{L}_3$ in 10^{-4} M CH_3CN solution as a function of wavelength.

440 nm in the presence of the metal ions. These bands are assignable to donor–acceptor charge transfer transitions. Metal free $\mathbf{L}_4$ exhibits a strong band around 365 nm along with a shoulder near 330 nm. Both these bands are of intramolecular charge transfer [18] from the NMe_2 donor end to the diaza-18-crown-6 which is a weak acceptor. Upon addition of a metal ion, the macrocycle becomes a good acceptor and two bands are observed whose position as well as ε_{max} values are sensitive to the nature of the metal. In Fig. 1, the charge transfer bands are clearly generated for $\mathbf{L}_4$ especially in the presence of Zn(II) and Cd(II). On the other hand, such intense charge transfer bands are only weakly observed for $\mathbf{L}_3$. It clearly indicates that donor acceptor interaction induced is larger for $\mathbf{L}_4$/Zn(II) compared to $\mathbf{L}_3$/Zn(II). However, these observations are not directly related to the TPA cross-section data, where $\mathbf{L}_3$ in the presence of Zn(II) gives the largest value.

3.2. Binding constant determination of metal complexes

The binding constants were determined from the variation of absorbance intensity at proper observation wavelengths for both the chromophores. A typical example of spectral change in case of $\mathbf{L}_4$, upon addition of metal salt is given in Fig. 2a, which clearly shows one isosbestic point corresponding to only one equilibrium process. Here, for the complexation of chromophores $\mathbf{L}_3$ and $\mathbf{L}_4$ with Zn(II) salts, the $\log K_s$ values were found to be 4.87 and 5.78,

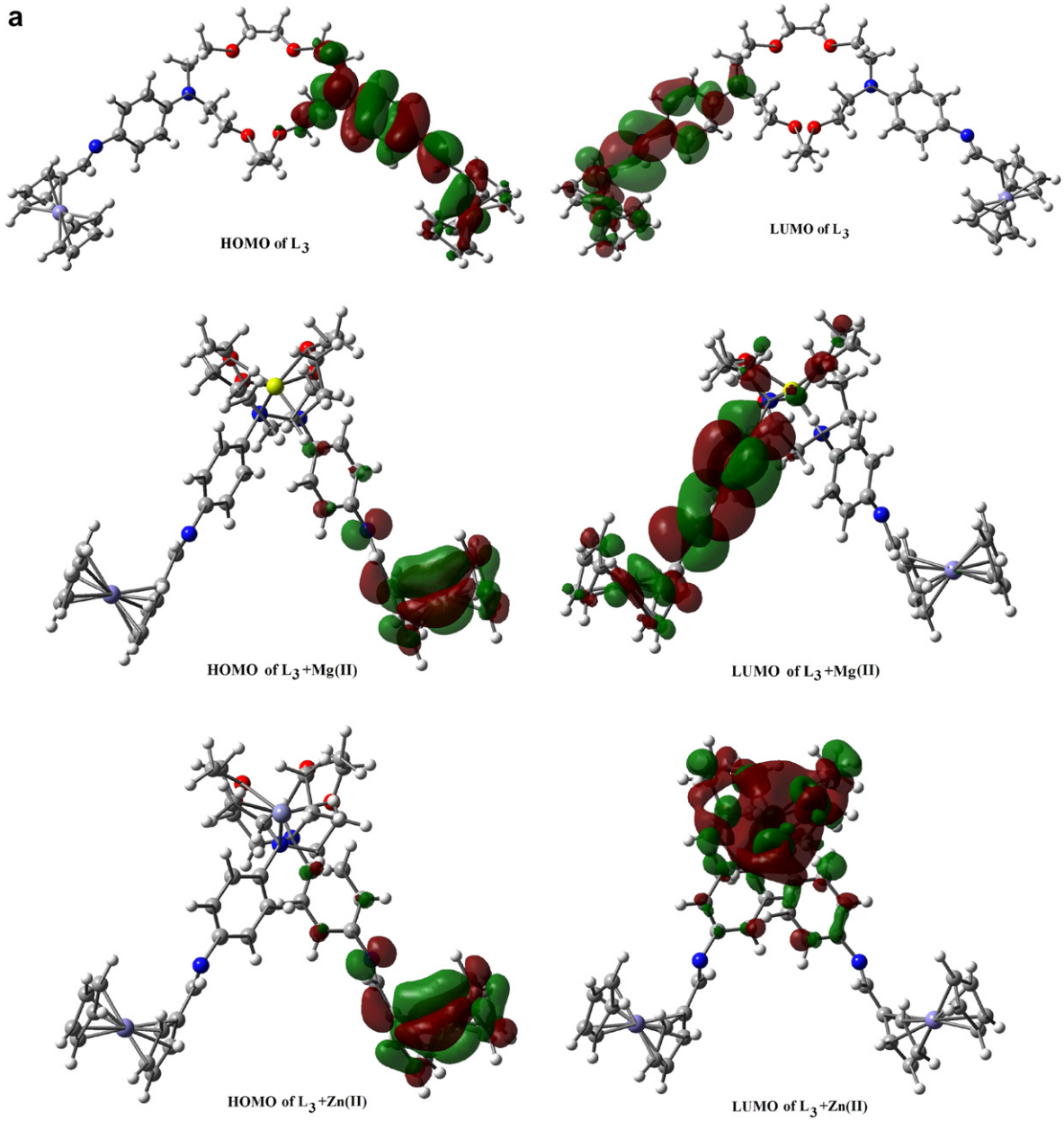

Fig. 5. Contour surfaces of HOMO and LUMO for the chromophores $\mathbf{L}_3$ and $\mathbf{L}_4$ and their corresponding Mg(II) and Zn(II) complexes.

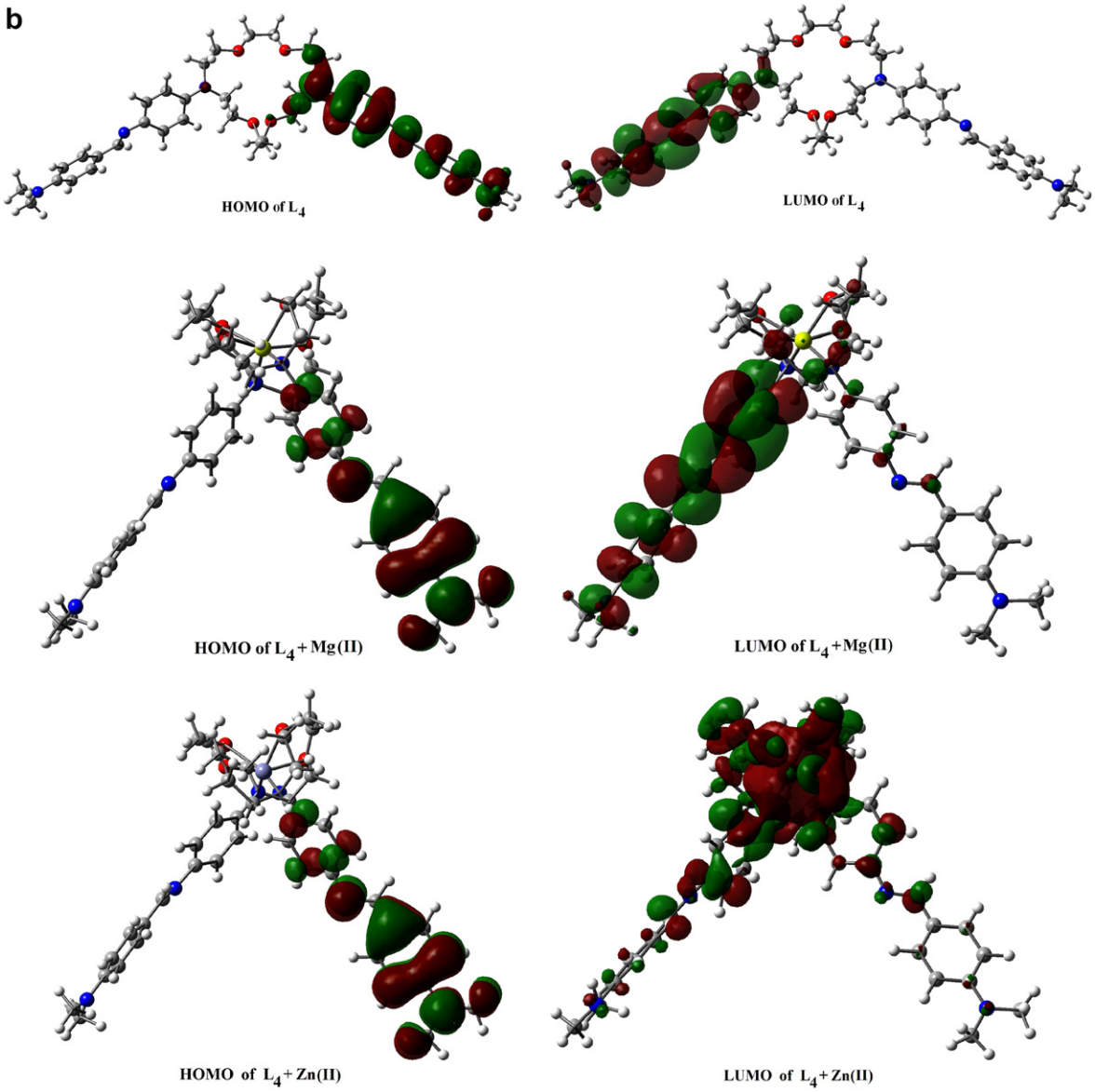

Fig 5. (*continued*)

respectively. And for Mg(II) complexes these values were 4.76 and 4.68, respectively.

3.3. Two-photon absorption

The TPA cross section (σ_2) measurements were carried out in the wavelength range, 750–850 nm which is within the window of minimum cell damage for any in vivo studies. The σ_2 values for $\mathbf{L}_3$, $\mathbf{L}_4$ alone and in the presence of metal ions are collected in Table 1. Metal free $\mathbf{L}_3$ and $\mathbf{L}_4$ do not show any significant TPA cross-section. In the presence of Na(I) or K(I) ion as input, the σ_2 value increases marginally in case of $\mathbf{L}_4$ but significantly in case of $\mathbf{L}_3$. This is commensurate with the fact that while *N*,*N*′-dimethylbenzene is a strong donor group, ferrocene is a good electron transfer group [19]. Other metal ions studied also corroborate this fact and show much higher σ_2 values with $\mathbf{L}_3$. It is also very clear that there is an increasing order of TPA cross-section value when we go through the alkali metal to alkaline earth metal and finally to the transition metal. It is certainly due to the effective nuclear charge of the metal ion that is increased in the same trend with greater extent of encapsulation in the aza crown ether receptor and hence they can communicate with the two side arms more effectively. Among the metal ions studied, Zn(II) shows the highest value of σ_2 in the wavelength range. The corresponding open-aperture Z-scan traces for $\mathbf{L}_3$ with Mg(II), Ca(II), Zn(II) and Cd(II) are given in Fig. 3.

We also recorded the change in TPA cross-section values as a function of wavelengths only for $\mathbf{L}_3$ (as this chromophore gave some significant σ_2 values in practice) in the presence of different metal ions. Interestingly, in every case there is a gradual increase of σ_2 value up to a certain limit

followed by dropping to a minimum (Fig. 4). All the photophysical data for the chromophores $\mathbf{L}_3$ and $\mathbf{L}_4$ and their different metal complexes are given in Table 1.

3.4. Theoretical studies

Geometry optimization has been carried out for the ligands ($\mathbf{L}_3$ and $\mathbf{L}_4$) and their Mg(II) and Zn(II) complexes. All calculations were performed by the GAUSSIAN 03 program [20] using the B3LYP functional [21] with 6-31G* (for C, H, N, and O) and LanL2DZ [22] (for Fe, Zn and Mg) basis set. When LanL2DZ basis set was used along with the 6-31G* basis set then Gen was used to designate this. This was chosen as a compromise between accuracy and applicability to a larger molecular system. All the optimized geometries possess the C1 symmetry. Experimentally, we found that when free chromophores ($\mathbf{L}_3$ or $\mathbf{L}_4$) coordinate with metal ions, the magnitude of the TPA cross-section increased. In case of $\mathbf{L}_3$ the change is much more extensive rather than the chromophore $\mathbf{L}_4$. The TPA cross-section is directly correlated with the extent of intramolecular charge transfer transition through π-bridge. Generally, the frontier molecular orbitals, especially HOMO−1, HOMO, LUMO and LUMO+1 play the significant role to electronic transition during two-photon absorption [10]. For more intuitional analysis of the influence of the metal ion upon TPA property, we should consider the contours of some correlative occupied and unoccupied frontier orbitals (Fig. 5).

From the contour surface diagrams it is clear that in free ligand both the HOMO and LUMO are situated in the side arms of the ligands, indicating only a $\pi \rightarrow \pi^*$ electronic transition (i.e., intra-ligand charge transfer, ILCT). Whereas, in metal complexes the HOMO is mainly concentrated on the π-conjugated side arm and LUMO resides on the metal atom (in case of Zn(II)) which clearly indicates that a strong intraligand charge transfer transition accelerated by metal atom, takes place after complexation. As Mg(II) ion has no diffused electron cloud like Zn(II) the LUMO is just shifted towards metal center rather than residing upon it like the former.

Here, in every case, it is worth noting that a more obvious increased intramolecular charge transfer transition triggered by metal ions is very beneficial to interpret the enhancement of TPA cross-section from the free chromophores [23]. Again from the energy level diagrams of the ligands it is clear that the energy of both HOMO and LUMO orbitals decrease significantly when both form complexes with metal ions, which indicates that an electronic charge delocalization takes place after complexation. As for example, we find from Fig. 6, the HOMO and LUMO energy of Mg(II) complex of chromophore $\mathbf{L}_3$, −8.43 eV and −5.35 eV (these are −8.46 eV and −6.19 eV respectively for the Zn(II) complex) is more stable than that of free chromophore ($\mathbf{L}_3$), which are −4.81 eV and −1.00 eV, respectively. Furthermore, it also accompanied with the decrease of HOMO–LUMO gap after complexation as expected, which are 3.81 eV for the chromophore ($\mathbf{L}_3$) itself and 3.07 eV for the Mg(II) complex (this is 2.26 eV for the Zn(II) complex). The similar trend is followed for the free chromophore $\mathbf{L}_4$ and its complex with Mg(II) (and also for Zn(II) complex). Fig. 6. consists of calculated frontier orbital energy data for 10 occupied molecular orbitals and 10 unoccupied molecular orbitals obtained by B3LYP/6-31G* and are plotted serially for comparison with free chromophores.

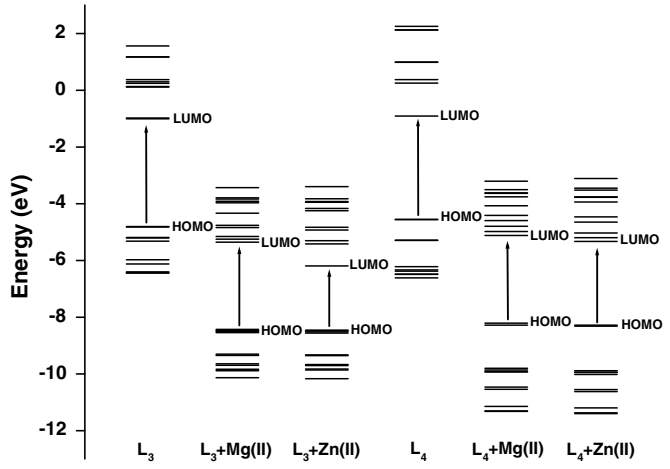

Fig. 6. B3LYP/6-31G* predicted molecular orbital energy levels for dipolar chromophores and their corresponding Mg(II) and Zn(II) complexes.

4. Conclusion

In this paper, the linear and nonlinear properties of two new dipolar chromophoric systems were studied in detail. The TPA properties have been also investigated using femto-second laser. The results reveal that there is an increasing order of TPA cross-section value from alkali metal ions to transition metal ions followed by alkaline earth metal ions depending upon the extent of binding with aza crown ether receptor which not only depends on the conjugation length, but also on the strength of the electron donor or acceptor property, which provide a rational design strategy for TPA molecules to fit in different applications. Overall, the effect of the alkali metals, alkaline earth metals and transition metals on the TPA cross-section was investigated. One crucial inference drawn from the present work is that the dipolar molecules can serve as a promising alternative TPA dyes for a variety of applications. Theoretical calculations at B3LYP functional with 6-31G* and LanL2DZ mixed basis set show clearly the shifting of charge density in the chromophores by metal ion incorporation into the cavity. Further studies on similar model systems are in progress in our laboratory.

Acknowledgements

Financial support received from CSIR, New Delhi, India to P.K.B. is gratefully acknowledged. D.G. thanks

DST, MCIT (India), and International SRF Program of Welcome Trust (U.K.) for the financial grant. A.J. and A.K.D. thank CSIR for their fellowship. We also thank Dr. Kousik Giri, School of Chemistry, University of Birmingham for his help regarding theoretical calculations.

Appendix A. Supplementary material

Supplementary data associated with this article can be found, in the online version, at doi:10.1016/j.jorganchem.2008.01.019.

References

[1] (a) W. Denk, J.H. Strickler, W.W. Webb, Science 248 (1990) 73;
(b) J.D. Bhawalkar, N.D. Kumar, C.F. Zhao, P.N. Prasad, J. Clin. Med. Surg. 37 (1997) 510.
[2] (a) G.S. He, G.C. Xu, P.N. Prasad, B.A. Reinhardt, J.C. Bhatt, R. McKellar, A.G. Dillard, Opt. Lett. 20 (1995) 435;
(b) G.S. He, J.D. Bhawalkar, C.F. Zhao, P.N. Prasad, Appl. Phys. Lett. 67 (1995) 2433;
(c) J.E. Ehrlich, X.L. Wu, L.-Y. Lee, Z.-Y. Hu, H. Roeckel, S.R. Marder, J.W. Perry, Opt. Lett. 22 (1997) 1843;
(d) M. Calvete, G.Y. Yang, M. Hanack, Synth. Met. 141 (2004) 231.
[3] (a) D.A. Parthenopoulos, P.M. Rentzepis, Science 245 (1989) 843;
(b) J.H. Strickler, W.W. Webb, Opt. Lett. 16 (1991) 1780;
(c) A.S. Dvornikov, P.M. Rentzepis, Opt. Commun. 119 (1995) 341;
(d) B.H. Cumpston, S.P. Ananthavel, S. Barlow, D.L. Dyer, J.E. Ehrlich, L.L. Erskine, A.A. Heikal, S.M. Kuebler, I.-Y.S. Lee, D. McCord Maughon, J. Qin, H. Röckel, M. Rumi, X.-L. Wu, S.R. Marder, J.W. Perry, Nature 398 (1999) 51.
[4] (a) Y.-F. Zhou, S.-Y. Feng, X.-M. Wang, J. Mol. Struct. 613 (2002) 91;
(b) Y. Ren, Q. Fang, W.-T. Yu, H. Lei, Y.-P. Tian, M.-H. Jiang, Q.-C. Yang, T.C.W. Mak, J. Mater. Chem. 10 (2000) 2025.
[5] B.L. Vallee, K.H. Falchuk, Physiol. Rev. 73 (1993) 79.
[6] (a) E. Ho, B.N. Ames, Proc. Natl. Acad. Sci. USA 99 (2002) 16770;
(b) H. Daiyasu, K. Osaka, Y. Ishino, H. Toh, FEBS Lett. 503 (2001) 1.
[7] A.Q. Troung-Tran, J. Carter, R.E. Ruffin, P.D. Zalewski, Biometals 14 (2001) 315.
[8] A.B. Chausmer, J. Am. Coll. Nutr. 17 (1998) 109.
[9] (a) Y. Suzuki, H. Komatsu, T. Ikeda, N. Saito, S. Araki, D. Citterio, H. Hisamoto, Y. Kitamura, T. Kubota, J. Nakagawa, K. Oka, K. Suzuki, Anal. Chem. 74 (2002) 1423;
(b) A. Takahashi, P. Camacho, J.D. Lechleiter, B. Herman, Physiol. Rev. 79 (1999) 1089.
[10] (a) S.J.K. Pond, O. Tsutsumi, M. Rumi, O. Kwon, E. Zojer, J.-L. Brédas, S.R. Marder, J.W. Perry, J. Am. Chem. Soc. 126 (2004) 9291;
(b) R. Bozio, E. Cecchetto, G. Fabbrini, C. Ferrante, M. Maggini, E. Menna, D. Pedron, R. Riccò, R. Signorini, M. Zerbetto, J. Phys. Chem. A 110 (2006) 6459;
(c) S. Das, A. Nag, D. Goswami, P.K. Bharadwaj, J. Am. Chem. Soc. 128 (2006) 402.
[11] H. Adams, R. Bastida, D.E. Fenton, B.E. Mann, L. Valencia, Eur. J. Org. Chem. (1999) 1843.
[12] M. Sheik-Bahaei, A.A. Said, T. Wei, D.J. Hagan, E.W. Van Stryland, IEEE J. Quantum Electron. 26 (1990) 760.
[13] (a) D. Kim, A. Osuka, M. Shigeiwa, J. Chem. Phys. A 109 (2005) 2996;
(b) H. Rath, J. Sankar, V. Prabhuraja, T.K. Chandrasekhar, A. Nag, D. Goswami, J. Am. Chem. Soc. 127 (2005) 11608.
[14] P. Sengupta, J. Balaji, S. Banerjee, R. Philip, G. Ravindra Kumar, S. Maiti, J. Chem. Phys. 112 (2000) 9201.
[15] (a) J. Bourson, J. Pouget, B. Valeur, J. Phys. Chem. 97 (1993) 4552;
(b) S. Das, A. Nag, K.K. Sadhu, D. Goswami, P.K. Bharadwaj, J. Organomet. Chem. 692 (2007) 4969.
[16] S. Fery-Forgues, M.-T. Le Bries, J.-P. Guetté, B. Valeur, J. Phys. Chem. 92 (1988) 6233.
[17] A. Caballero, A. Tárraga, M.D. Velasco, P. Molina, Dalton Trans. (2006) 1390.
[18] P.R. Bangal, S. Chakravorti, J. Photochem. Photobiol. A 116 (1998) 191.
[19] S. Barlow, S.R. Marder, Chem. Commun. (2000) 1555.
[20] M.J. Frisch et al., GAUSSIAN 03, Revision B.03 Gaussian, Inc., Wallingford, CT, 2004.
[21] (a) A.D. Becke, J. Chem. Phys. 98 (1993) 5648;
(b) R.-P. Òscar, Y. Luo, H. Ågren, J. Chem. Phys. 124 (2006) 94310.
[22] (a) P.C. Hariharan, J.A. Pople, Chem. Phys. Lett. 16 (1972) 217;
(b) P.J. Hay, W.R. Wadt, J. Chem. Phys. 82 (1985) 299;
(c) P.J. Hay, W.R. Wadt, J. Chem. Phys. 82 (1985) 270;
(d) W.R. Wadt, P.J. Hay, J. Chem. Phys. 82 (1985) 284.
[23] Q. Zheng, G.S. He, P.N. Prasad, J. Mater. Chem. 15 (2005) 579.